

Insulation Materials: Testing and Applications, Third Volume, ASTM STP 1320, R. S. Graves and R. R. Zarr, Eds., American Society for Testing and Materials, 1997.

## Laboratory Procedures for Using Infrared Thermography to Validate Heat Transfer Models

Daniel Turler, Brent T. Griffith, and Dariush K. Arasteh

Windows and Daylighting Group  
Building Technologies Department  
Environmental Energy Technologies Division  
Ernest Orlando Lawrence Berkeley National Laboratory  
University of California  
1 Cyclotron Road  
Berkeley, CA 94720

June 1996

# Laboratory Procedures for Using Infrared Thermography to Validate Heat Transfer Models

Daniel Türler Brent T. Griffith, and Dariush K. Arasteh  
Windows and Daylighting Group  
Ernest Orlando Lawrence Berkeley National Laboratory  
University of California  
1 Cyclotron Road  
Berkeley, CA 94720

## Abstract

Infrared (IR) imaging radiometers, which measure relative levels of thermal radiation energy, can be used for noninvasive surface temperature measurements of building thermal envelope components undergoing steady-state heat flow in laboratory thermal chambers. One advantage of IR measurement is that it provides large contiguous sets of surface temperature data which are useful for validating the accuracy of complex computer models that predict heat flow through thermally insulated systems. Because they give such detailed information about surface temperature, IR measurements complement hot-box measurements of heat flow. This paper recommends general procedures for reliable quantitative thermographic measurements in chambers operated for winter heating conditions. Actual surface temperature depends on heat flow, surface emittance, and environmental conditions such as air temperature, air flow field, and background thermal radiation. The infrared temperature measurements are affected by many of the same factors including surface emittance, air temperature, background thermal radiation, and air humidity. Equipment specifications for the absolute accuracy of infrared temperature measurements are typically  $\pm 1^\circ$  to  $\pm 2^\circ\text{C}$ . Measurements that use a temperature-controlled reference emitter to remove error appear to show accuracies of  $\pm 0.5^\circ\text{C}$  for flat specimens with low temperature gradients.

## Introduction

With quantitative data on thermal performance designers can make informed decisions about a building's thermal envelope specifications. The thermal performance of building components is measured in the laboratory using hot-box methods described in American Society for Testing and Materials (ASTM) literature [1, 2, 3]. These tests yield overall values for thermal transmittance under steady-state environmental conditions. Because of the time and cost associated with physical testing, thermal performance is commonly modeled by computer programs under idealized thermal boundary conditions that correspond to hot-box tests. One example is the U.S. effort to rate and label fenestration products which uses mostly computer simulated data. Computer simulation programs vary widely in complexity. Sometimes complex programs are used to develop correlations for and to validate the accuracy of simpler programs. Complex programs use finite-element or finite-difference methods to solve in two or three dimensions for energy flows occurring principally by conduction; these programs also solve for fluid flows to determine convection and for view factors to determine thermal radiation.

As computer programs and building components evolve and incorporate new features and complexities, more detailed methods of validating the accuracy of the computer models become useful. The accuracy of heat flows predicted by computer programs has gained acceptance largely by comparison to hot-box testing. Surface temperature is another physical phenomena that can be measured directly and compared to computer simulation results. Surface temperatures are also closely related to heat flows. Though heat flow is closely linked to energy use, other thermal characteristics such as condensation and thermal comfort are closely linked to surface temperatures. Also, surface temperature data can help identify the local effects of

small changes in subcomponents (such as structural members) of an insulated building component; these effects may not be measurable by changes in overall heat flow. Computer simulations that model convection and radiation, in addition to conduction benefit especially from comparing local thermal phenomena rather than only overall heat flows.

Infrared thermography is a noninvasive technique for measuring large amounts of surface temperature data. The technique uses relative measurements of infrared thermal radiation energy. Thermal radiation is one type of electromagnetic radiation that is continuously emitted by all substances due to molecular and atomic agitation associated with the internal energy of the material. A previous set of publications [4, 5, 6] describes infrared thermographic measurements and computer modeling of insulated glazing units and offers an opportunity to compare thermographic data from two different laboratories that measured separate but identical building component specimens. Although there was fairly good agreement between experimental and computer data in these studies, they showed that a general procedure for infrared thermography may improve the accuracy of measurements.

This paper discusses general procedures for using infrared thermography to measure surface temperatures of flat building component specimens in thermal chambers operated similarly to hot-box tests for winter heating conditions. The procedures are designed to minimize error in infrared temperature measurements for research efforts that quantify surface temperatures in order to compare them to computer simulated data. This paper relies on existing hot-box test standards to specify many details of a complete measurement procedure. We focus only on flat surfaces because of complexities in accounting for background radiation when a specimen has self-viewing surfaces that extend perpendicular to the test plane. Other existing ASTM standard practices discuss use of infrared thermography in the field, infrared imaging equipment performance, and useful terminology [7,8,9].

The first appendix to this paper documents details of infrared measurements at the authors' laboratory (IRLab). It focuses on examples of IRLab equipment and sample results from error analysis of infrared temperature measurements.

## Equipment

To measure a flat building component in thermal chambers under winter heating conditions, two chambers, a climate chamber and a thermography chamber, are recommended to generate steady-state heat flow across the test specimen. Thermographic measurements should be conducted on the side of the specimen that faces the thermography chamber. The usual instrumentation associated with hot-box tests should be used, along with a calibrated transfer standard (CTS), an infrared imaging radiometer (imager), a background mirror, a reference emitter, and an air dryer. Figure 1 shows the general layout.

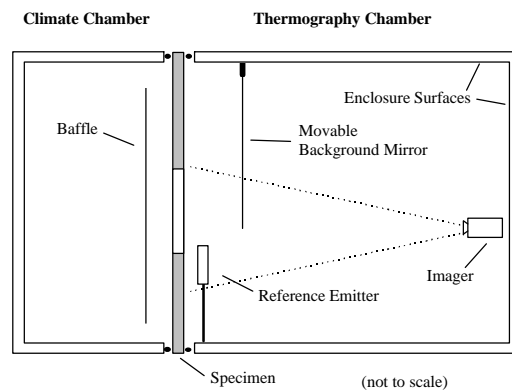


Figure 1. General Arrangements of Thermography Chamber and Climate Chamber

### *Climate Chamber*

Arrangement, construction, instrumentation, and air circulation and conditioning equipment of the climate chamber may be the same as specified for a climatic chamber in the ASTM Test Method for Thermal Performance of Building Assemblies by Means of a Calibrated Hot Box (C 976) section 5.4 [1], or for a cold box in ASTM Test Method for Steady-State Thermal Performance of Building Assemblies by Means of a Guarded Hot Box (C 236) section 6.4 [2].

### *Thermography Chamber*

A thermography chamber allows for control and measurement of air temperature and velocity on one face of a specimen under uniform thermal radiation conditions while also enabling an infrared imager to measure the specimen. The main difference between a thermography chamber and a metering chamber used in hot-box testing is that a thermography chamber must be designed for an unobstructed view of the specimen and therefore cannot employ a baffle in the same fashion as a hot-box. For certain specimens, it is necessary to dry the air in order to avoid surface condensation, which will alter surface emittance and affect performance. The usual arrangement of the chamber consists of five or more sides with internal dimensions matching the opening of the climate chamber. The interior surfaces of the chamber that view the specimen are referred to as the enclosure surfaces. The geometry of the enclosure surfaces should accommodate the viewing distance required by the infrared imager. Although close-up views of a specimen may be taken from a distance of as little as 1 m, imaging one square meter of the specimen may require a viewing distance of 4 m. The imager may be located in the air space between the enclosure surfaces and the specimen, or it may be situated to view through ports in the enclosure surface(s). All of the necessary cooling, heating, and air circulation equipment should be located behind enclosure surfaces. Heat transfer through the thermography chamber walls should be kept small and uniform. Avoid thermal bridges and air and moisture leaks through the chamber walls. The enclosure surfaces should be instrumented with surface temperature probes, and the surface material should be diffusely reflecting with emittance of more than 0.8. The temperature of the enclosure surfaces will determine both background infrared thermal radiation and also the radiation component of the surface conductance.

Air circulation and conditioning require special consideration. Design considerations include maintaining uniform (and appropriate levels of) surface conductance, maintaining spatially uniform and well-controlled air temperatures, and replicating conditions found in normal hot-box testing. These considerations are complicated by the large distance necessary between the specimen and enclosure surfaces in contrast to the baffle configuration used in a hot-box. The true surface temperatures, which are to be measured with the infrared thermography equipment, depend strongly on the surface conductance (film coefficient). Natural convection or fan-assisted natural convection should be used to approach the desired mean surface conductance. Periodic air velocity measurements should be made across the width of a uniform maskwall, out of the boundary layer, about 75 mm off the surface. Air velocity should be monitored and recorded during any test and should never exceed 0.5 m/s near the specimen surface outside the boundary layer. More research is needed to determine the required level of air velocity uniformity. An air velocity probe should be mounted in a representative location that does not obstruct the imaging system field of view. Air supplied to the test specimen surface has to be uniform in temperature across the width of the specimen and over time to ensure steady-state operation. It is suggested that an air sink be located across the entire bottom of the specimen to retrieve air cooled down by natural convection. Multiple, individually controlled zones across the width should be used to control air temperature. Cooling equipment may be used in a thermography chamber to extract heat.

### *Infrared Thermography System*

Infrared thermography equipment uses an infrared imaging radiometer to generate images based on surface temperatures and quantifies temperature by correcting for emissivity and background radiation. Two types of infrared imagers are scanners and array devices. A scanner uses a single detector and a system of

mirrors to scan the field of view (FOV), array devices use a matrix of detectors to resolve parts of the FOV individually. Different imagers also measure different wavelengths of thermal radiation. Short-wave imagers measure in the 3 to 5  $\mu\text{m}$  range; long-wave imagers measure in the 8 to 12  $\mu\text{m}$  range. Short-wave systems can be less expensive than long-wave systems; however, short-wave systems are not suitable for many fenestration components because of infrared transmission can be up to 80% through glass in these wavelengths. Postprocessing software does not compensate for infrared transmittance. Hence, long-wave imagers are more suitable for testing all types of building components. Because array devices are currently only available with short-wave detectors, we focus on long-wave, scanning-type imagers. Various infrared temperature measurement devices exist that are not imaging systems but measure data from single points or along a single line. Some procedures discussed here may be adapted for use with such point and line-scanner devices to yield useful infrared measurements.

An infrared thermography system used to gather surface temperature data should be selected for its spatial and thermal resolution. Two parameters are used to quantify the basic performance of the infrared imager, the *instantaneous field of view* (IFOV) and the *minimum resolvable temperature difference* (MRTD) [8, 9]. It is recommended that fairly high resolution equipment with less than 2 milliradians for the IFOV value and less than 0.2°C for the MRTD be used. The infrared scanner makes multiple measurements of infrared energy across the field of view (FOV) and combines them into a single image. Each measurement made by the scanner's detector is sized by the IFOV. Systems typically produce thermograms at a resolution that is higher than the actual number of IFOV to improve imaging quality. Therefore take care when interpreting the apparent resolution of text data. The field of view is basically the sum of the available IFOVs; it will determine the viewing distance and area that can be imaged. A broad field of view allows a shorter distance between the test specimen and the imager but can introduce perspective distortions that decrease spatial accuracy. At a given resolution, increasing the FOV by using expanding optics will increase the effective IFOV, resulting in lowered resolution. It is recommended that the infrared imager be specially calibrated with a higher concentration of points in the temperature range of interest for building components and the field conditions under which they are used.

For quantitative thermography, infrared imagers usually need to be combined with ancillary, computer-based processing hardware and software. The thermography computer typically uses an analog-to-digital converter to capture analog thermograms; future imagers may pass data to a computer in an entirely digital format. Standard capabilities should include: averaging data over time, correcting for emissivity and background, and transferring selected temperature data from thermograms to text files. Postprocessing of infrared data involves using the specialized thermography computer along with subsequent analysis and plotting of text data in separate software such as a spreadsheet.

#### *Background Radiation Mirror*

Accurate infrared thermography requires collecting data on the level of background radiation. A highly reflective mirror should be used to measure background radiation with the infrared imager. The background radiation level is used with the specimen surface emittance to calculate the fraction of the reflected background radiation that should be subtracted from the infrared imager's measurement of specimen radiosity. Aluminized polymer films with an emittance of about 0.03 are a good choice for mirror material. The mirror should be large enough to capture a representative portion of the background. Remote actuation is useful for positioning the mirror in front of the test specimen or stowing the mirror when it is not in use. The mirror should be stowed so that the reflective side is hidden; the thermography chamber's enclosure surfaces can then remain diffusely reflecting with emittance of more than 0.8.

#### *Reference Emitter*

Previous research by the authors [10] showed the effectiveness of using external reference emitters to increase the accuracy of thermographic measurements. A reference emitter is a temperature-controlled

device with a known surface emittance. During each measurement, the reference emitter is parallel to the specimen's surface in the FOV of the infrared imager. The reference emitter should stay reasonably in focus while the imager is focused primarily on the test specimen. The reference emitter should be designed and placed so that its presence interferes minimally with air temperature and flow results. The temperature of the reference emitter is measured and recorded with a temperature probe; an absolute accuracy of  $\pm 0.04^{\circ}\text{C}$  or better is recommended. The temperature controller should provide temperature stability of  $\pm 0.02^{\circ}\text{C}$  and a range of temperatures similar to the test specimen's expected range of surface temperatures. The surface temperature of the reference emitter should be determined with an absolute accuracy of  $\pm 0.15^{\circ}\text{C}$  or better. The reference emitter can have a near blackbody surface with emittance of 0.95 or higher or the same surface material as the test specimen.

Blackbody extended-area reference emitters are available commercially. Such units are used to calibrate thermography equipment and to determine MRTD. One design uses thermoelectric (Peltier effect) heat pumps for heating or cooling the reference surface with a fast response time (several seconds). The reference surface may be made of a solid aluminum or copper plate with a special paint having an emittance that averages 0.97 over 8 to 12  $\mu\text{m}$ . Depending on the temperature difference between the reference emitter surface and the ambient, the thermoelectrics require substantial heat exchange with the surrounding ambient. Waste heat and/or exhausted air should not be released inside the thermography chamber. Thus, bulky ducting may be necessary with commercial devices.

A second approach is to fabricate a reference emitter based on a temperature-controlled liquid system. Using a refrigerated bath/recirculator to control the temperature of a highly conductive plate can yield an effective external emitter that may be less disruptive to chamber conditions than air-based commercial devices. A custom device can be finished with a thin surface layer of the same material as that of the specimen being measured. The emitter plate should have an insulated design for an isothermal front surface and minimal disruption to the radiation environment inside the thermography chamber on its remaining sides.

#### *Air Dryer*

Moisture condensation on the surface of the specimen being imaged must be avoided as it will alter the emittance and change the infrared radiation characteristics. The dew point temperature of the air in the thermography chamber has to be lower than the lowest surface temperature of the test specimen. An air drying system to lower humidity can be built into the thermography chamber or hooked up externally with ducts or flexible hoses. The dryer's impact on the air temperature and velocity uniformity must be kept minimal. One method to dry air is to run it through a tank filled with desiccant; the desiccant will need to be regenerated periodically. Another method is to cool the air below the dewpoint, condensing out moisture, and then reheating the dried air.

#### *Direct Contact Temperature Instrumentation*

Section 5.7 of ASTM C 976 describes the location and installation of temperature sensors in climate and metering chambers. To the extent possible, this practice also applies to a thermography chamber. One or more thermocouples are installed on each enclosure surface of the thermography chamber and the maskwall as described in ASTM C 236 section 6.5.1. At least two warm-side air temperature sensors have to be located in close proximity to but outside the boundary layer. The sensors should be located at the top and bottom of the maskwall plane and parallel to it. If multiple zones are being controlled a pair of sensors should be located in each zone. Cold-side specimen surface temperature sensors may be installed as described in section 5.7.1. of ASTM C 976.

#### *Calibration Transfer Standard*

A calibration transfer standard (CTS) is a large area heat flux transducer used to determine surface conductances. The device, procedures, and calculations are described in sections 5 and A1 of ASTM Test

Method for Measuring the Steady State Thermal Transmittance of Fenestration Systems Using Hot Box Methods (C 1199) [3]. Surface conductance values must be obtained with temperature data for useful comparison to computer models. The CTS gives the information needed to calculate mean surface conductance. A CTS is also very useful for verifying thermographic measurements by direct comparison of infrared data to the CTS's direct contact data. ASTM C 1199 is for fenestration testing; CTS designs may need to be altered for other types of building assemblies.

### **Specimen Preparation**

Preparing a building component specimen for thermography is somewhat similar to hot box testing, with differences in flush mounting and emittance modifications. Large area specimens can simply be located between the chambers with perimeter insulation. The maximum size of the test specimen is determined by the chamber openings and the edge effects on air flow and temperature from the enclosure surfaces. A close-fitting, foam maskwall holds smaller specimens and separates the chambers. The maskwall thickness should be similar to or thicker than that of the test specimen so that all four sides of the test specimen are entirely covered. The specimen surface facing the thermography chamber should be mounted flush with the maskwall. Unless infiltration is being investigated, specimens should be sealed for air tightness as described in section 6.1.4 of ASTM C 976.

Specimens with a surface emittance of less than 0.8 should be covered with a minimal thickness of material to raise the surface emittance to more than 0.8. The material should be selected to minimize change in the specimen's thermal performance although some change in thermal radiation is unavoidable. This attention to surface emittance is necessary for accurate temperature measurements because surfaces with low emittance (high reflectance) are very sensitive to errors in emittance and background radiation corrections.

The specimen should be prepared with low-emittance location markers, which will help identify spatial locations and distances in the thermographic data. Location markers should be thin and firmly adhered to the surface; a useful size is approximately 3 mm wide and 20 to 50 mm long. Aluminum tape is a good choice, but care should be taken to avoid altering the specimen's performance with high conductivity tape. Aluminized polymer films may also be used. Reflective markers show background radiation and will be identifiable in the data only when the background has a different effective temperature than the surface. When data are merged from different imager views, the markers indicate how to join the images. Nonhomogenous features of interest and center lines should be marked outside of the exact region to be measured and in such a fashion that real specimen distances can be measured for subsequent synchronization with the thermographic data. This step is critical to obtaining accurate spatial coordinates to pair with infrared temperature data.

### **Test Chamber Calibration**

A separate measurement should be conducted using a CTS to characterize and adjust the surface conductances present in the thermal chambers. CTS test procedures and data analysis are given in section 5.2. of ASTM C 1199. The CTS size and conductance should be close to that of the specimen(s) being measured. The chambers should be adjusted to obtain mean surface conductances within 5% of the desired standard values (e.g., for fenestrations, 30 W/m<sup>2</sup>·K for the cold side and 8.3 W/m<sup>2</sup>·K for the warm side as described in ASTM C1199, Section 7.1.10). Because there is no baffle in the thermography chamber, radiation is directly or indirectly exchanged with all the enclosure surfaces. Therefore the radiative heat transfer calculation is complicated; it is a form factor analysis, described in section A2.1 of ASTM C 1199. Depending on temperature uniformity, emittance, and geometry, it may be necessary to perform the calculation for six or more surfaces. In addition to the calculations described in ASTM C 1199 which use the average temperatures from the CTS, it is useful to analyze each individual pair of warm side and cold side temperatures, checking for horizontal variations of surface conductances and spatial uniformity of the

heat flux. Data can be gathered from individual locations for direct comparison to infrared thermography data. Infrared measurements should be made on the CTS to aid in verifying imager performance.

## Procedure

### *Surface Emittance Determination*

The specimen's emittance should be measured in a separate experiment that compares it to the emittance of known material. This emittance value can then be used in subsequent infrared measurements. The true surface emittance depends on the specimen material, its surface condition, and the temperature. The correct emittance value will vary with the type of infrared imager. To make use of literature values for emittance, it is necessary to obtain spectral data and weight the wavelength-dependent reflectance with the wavelength-dependent detector response over the range of wavelengths being measured. Even if this analysis can be performed (which is unlikely for diffuse materials), it is still recommended to measure the value as described below to compensate automatically for the spectral response of the infrared system being used.

To conduct the emittance measurement, thin specimens of both a known material and the unknown sample material, should be brought to the same surface temperature by mounting in good thermal contact to an isothermal, temperature-controlled plate. The temperature should be set approximately 10° to 20°C above or below the background temperature to insure high contrast between the radiosity from the specimens and the radiation from the background. The infrared imager should be set to emittance 1.0 to turn off any background radiation compensation; select the finest resolution units. Both specimens should be imaged simultaneously. Readings should be averaged over both time and space for the equivalent blackbody temperature of the unknown sample,  $T_{e=1,smpl}$ , and the equivalent blackbody temperature of the known reference material,  $T_{e=1,ref}$ . Background radiation equivalent blackbody temperature,  $T_{back}$ , is quantified in the same units using a background mirror. Caution must be exercised to provide a very uniform background, which may be verified by imaging the background mirror. The emittance of the sample material,  $e_{smpl}$ , is then calculated from the emittance of the known material,  $e_{ref}$ , using equation 1. Several measurements should be made and then averaged.

$$e_{smpl} = \frac{\left( T_{e=1,smpl}^4 - T_{back}^4 \right)}{\left( T_{e=1,ref}^4 - T_{back}^4 \right)} e_{ref} \quad (1)$$

Theory for Equation (1) -- Equation 1 may be derived from equations 2 through 5. Equations 2 and 3 are usual expressions for total radiosity emanating from each surface. Algebraic combination and reduction of these two equations starts by eliminating the blackbody emissive power,  $E_b$ , shown in equation 4 where the Stefan-Boltzmann constant,  $\sigma_{SB}$ , is multiplied by surface temperature,  $T$ , to the fourth power. Equation 5 defines an equivalent blackbody temperature of a surface,  $T_{e=1}$ , that would yield a blackbody emissive power equal to the radiosity from a surface,  $J_{surf}$ . To apply these equations, the following assumptions are made: (1) Both the reference material and the unknown specimen are opaque so that the sum of emittance and reflectance equals unity. (2) Directional variations in emittance are negligible. (3) The surface temperatures of the two materials,  $T$ , are the same because they are both mounted on a highly conductive, isothermal plate. (4) Both materials are subject to the same background thermal radiation. (5) The variation in spectral emittance is negligible over the temperature range of -20°C and 50°C.

$$J_{ref} = e_{ref} E_b + (1 - e_{ref}) G_{back} \quad (2)$$

$$J_{smpl} = e_{smpl} E_b + (1 - e_{smpl}) G_{back} \quad (3)$$

$$E_b = \epsilon_{SB} T^4 \quad (4)$$

$$J_{\text{surf}} = \epsilon_{SB} T_{e=1}^4 \quad (5)$$

### *Chamber Operation*

The prepared test specimen assembly should be mounted between the climate and thermography chambers. An airtight fit minimizes accumulation of moisture in the chambers. The specimen orientation and direction of heat transfer should match field use conditions. Setpoint temperatures of -17.8°C (0°F) on the cold side and 21.1°C (70°F) on the warm side are commonly used for winter heating conditions. Air-flow settings should be based on those determined by prior chamber calibration with the CTS. Environmental conditions are maintained for a length of time sufficient to ensure that heat flow through the specimen is at steady state. Because individual thermograms are recorded over a period of time measured in minutes or seconds, any cycling to control chamber temperatures should occur at a rate faster than the infrared measurement time. A graphical display of warm and cold side temperatures should be monitored with an update interval that is at least 10 times faster than the overall recording time of one thermogram.

### *Infrared Imaging*

The infrared imaging system should be positioned as close to the specimen as is practical, allowing the imager to view the desired portion of the specimen, the reference emitter, and at least two location markers, and also allowing the background mirror to be deployed. Each thermogram should include enough of the reference emitter to provide at least 10 horizontal and 10 vertical infrared elements or IFOVs. How much of the specimen is selected for viewing will vary depending on the specimen's geometry and thermal contrast; small features and high surface temperature gradients require close viewing. The maximum viewing distance to resolve a given feature is determined by the IFOV of the infrared imaging system where three to five (or more) IFOVs are needed to resolve the temperature of a feature. The temperature span of the infrared imaging system should be the smallest possible value that includes all the features of interest. The reference emitter surface temperature should be set to within  $\pm 3^\circ\text{C}$  of the temperature of a given feature of interest. Thermograms should be recorded by averaging data over time, usually by averaging multiple frames of data. For analog systems, 20 frames or more is recommended. Depending on the range of temperatures present it may be necessary to record several thermograms with smaller temperature spans and varying center temperatures. When multiple images with different spans and center temperatures are taken of the same view, good data alignment can be insured by including at the time of capture geometry overlays that will be used for postprocessing in all the related thermograms. Immediately before and/or after imaging a particular view of the specimen, deploy the reflective background mirror parallel to and in front of the test specimen and record the effective background radiation level (emittance set to 1.0). The imager viewing angle is usually at an offset from normal to prevent reflections of the cold scanner lens, which is an unavoidable nonuniformity in the background.

### *Data Recording*

Data on environmental conditions should be gathered with a computerized data acquisition system and should resolve complete sets for multiple bins of time covering the duration of the measurements. Each data set should include chamber air temperatures, air velocities, baffle temperatures, direct contact specimen surface temperatures, enclosure surface temperatures, maskwall temperature, and the reference emitter temperature. In addition it is suggested to monitor and record the air humidity inside the thermography chamber and note whether or not any condensation was visible. A log book should be used to identify the specimen, date, time of day, viewing distance, viewing angle, and all file names used to store data.

### **Data Processing**

### *Environmental Data*

The environmental data gathered by the data acquisition system can verify that measurements were made under steady-state conditions and indicate surface conductances and air temperatures. If conditions were steady state, multiple time-bins of data for the duration of the thermographic measurements can be averaged to one data set for surface conductance analysis. In addition, individual zones of cold- and warm-side air temperatures are averaged to one, bulk, warm-side air temperature and one, bulk, cold-side air temperature.

It is important to reevaluate mean surface conductances for the specimen as tested because the values are likely to differ from the CTS measurements conducted beforehand to calibrate the chambers. Computer models typically use mean surface conductance for boundary conditions; the appropriateness of a comparison of surface temperatures will depend largely on whether or not the surface conductances between the simulated and measured data are comparable. In the absence of metered heat flows, however, determining mean total surface conductances is not straightforward and is the subject of ongoing research. The cold-side radiative surface conductance may be calculated according to section 5.2.2.5 of ASTM C 1199. The warm-side radiative surface conductance may be calculated as outlined in section A2 of ASTM C 1199. Previous research by the authors [6] describes a method for estimating an average, convective warm-side surface conductance based on the average surface temperature of a flat specimen and literature correlations for constant heat flux. These calculations can also be verified using CTS data. Future research will address local film coefficients and improved ways to determine mean surface conductances. Local film coefficients could also be determined from air velocity measurements in the boundary layer.

### *Infrared Data*

To obtain useful quantitative surface temperatures, thermograms should first be corrected for emittance and background. Data should then be extracted from the thermogram as appropriate arrays of text values and synchronized with spatial coordinates. Compare infrared temperatures for the reference emitter to direct contact measurements and deviations should be used to scale the rest of the infrared data. Several data sets can be merged together, for example, to combine data from different views. If data from several different thermograms are merged, the environmental data must be checked for stability during the time that the different thermograms were taken.

Thermograms should be processed and text data produced with the thermography computer. The operator should input emittance using the correct, previously measured value. Input background radiation level as measured at the time the thermograms were recorded. This level is determined by an area and time average of the background mirror surface with emittance set to 1.0. Text data arrays extracted from the thermogram should be selected to cover the specimen regions that best correspond to the section being modeled by computer. The usual process is to use a geometric overlay to identify the selected region in the thermogram; software features allow transfer of data to text files. Images of location markers are used to identify regions so that specimen distance can be assigned to the array of temperature data. Usually the array of data will extend between overlay lines that are centered on location markers although data from location markers should not be used. It is recommended that data collected perpendicular to the main direction of the array be averaged as long as temperature gradients are largely one-dimensional.

The average temperature of the reference emitter surface is obtained by averaging thermogram data over an isothermal section of the emitter. Emittance and background are adjusted according to the type of reference emitter and background radiation and apparent temperature is recorded. The apparent reference emitter temperature is compared to the reference emitter temperature that was recorded by the data acquisition system using direct contact sensors. The reference emitter surface temperature may need to be adjusted from substrate measurements to account for heat flow and temperature gradients through the surface material. The difference between the apparent reference emitter temperature,  $T_{IR,Ref}$ , (as measured by

infrared) and the direct contact measured value,  $T_{DC,Ref}$ , should then be applied to correct the apparent sample surface temperature,  $T_{IR,smpl}$ , to arrive at the final surface temperature result,  $T$ , as shown in equation 6. This correction should be carried out for each temperature datum and for each thermogram and may be made using a spreadsheet. The correction described in equation 6 is for relatively small ( $<5^{\circ}C$ ) deviations amongst all temperature values. If larger ranges of temperature values need to be corrected, then a more complicated process should be used which uses radiation energy levels where temperature values would be raised to the fourth power.

$$T = T_{IR,smpl} - (T_{IR,Ref} - T_{DC,Ref}) \quad (6)$$

Final data sets should pair location coordinates with temperature values. The real distances between the location markers on the specimen are measured and a coordinate system is chosen to create temperature/location data pairs. The number of temperature values in the text array is evenly divided across the real distance to obtain an incremental distance that separates temperature values. Temperature data is then made into a function of x or y spatial coordinates mapped to the desired coordinate system. The form of the final data sets obtained for comparison to computer simulated data will depend on whether the simulation is two-dimensional or three-dimensional. For the two-dimensional simulations, the data sets will have the form (T, x) or (T, y) where T is the temperature at location x for horizontal data sets or at location y for vertical data sets. Similarly for the three-dimensional simulations, data sets will have the form (T, x, y).

#### *Error Analysis*

It is critical that uncertainty be estimated for the experimental data in order to accurately determine agreement with computer simulated data. Our focus is on methods for analyzing infrared data because of the complex nature of the infrared thermography system. Uncertainty also needs to be assigned to environmental data values; however, this analysis should be straightforward. The accuracy of surface temperature values from infrared thermographic data depends on both the characteristics of the imaging system and the techniques used to record and process thermograms. Infrared thermography systems typically have accuracy specifications of  $\pm 1.0^{\circ}$  or  $\pm 2.0^{\circ}C$ . The test procedures presented in this paper are intended to improve on this level of accuracy in order to improve its usefulness for validating computer models. This section therefore describes methods for determining the uncertainty of *referenced* infrared temperature measurements.

The temperature error analysis is divided into four parts. The first part addresses random errors that stem from the basic system “noise” level of the imager including optics, scanning, electronics, and emission and detection of infrared radiation. The second part involves errors arising from the necessary compensation for emittance and background thermal radiation. The third part considers systematic errors that arise from variations in the imager’s performance across the field of view. The fourth part combines the different types of error to arrive at an overall uncertainty estimate for thermographic surface temperature data.

Random Noise--The level of uncertainty arising from random noise error depends strongly on how thermographic data are averaged over time and space. Capturing and averaging multiple frames of data decreases the effect of random error. Thermography equipment specifications for the Noise Equivalent Temperature Difference (NETD) provide useful information on the level of random error. However, in many cases the NETD specification may not apply to the measurements because of the method of averaging used. Random error levels can be determined by conducting ancillary experiments with a temperature-controlled, isothermal surface -- usually a reference emitter. The isothermal plate should be measured with the imager using the same span as that used during the measurement being analyzed for errors. Basic random error can be assessed by capturing a single frame of data (no time averaging) and then analyzing every pixel, or thermographic data point, that lies within the region of the reference emitter and can be assumed to be isothermal. This basic level of random error can be described by the standard

deviation,  $\sigma_p$ , of each pixel-based temperature datum,  $t_p$ , and is calculated using equation 7. The mean temperature,  $t_m$ , is a spatial average of all the temperatures  $t_p$  and  $N$  is the number of pixels evaluated.

$$s_p = \sqrt{\frac{1}{N} \sum_{p=1}^N (t_p - t_m)^2} \quad (7)$$

The uncertainty in an individual temperature datum because of random error,  $\delta t_{p,ran}$ , depends on the number of frames averaged over time,  $n$ . It is recommended to conduct additional ancillary experiments that measure the isothermal plate with different numbers of frames averaged over time. The random errors typically do not follow a normal distribution, so it is recommended to multiply the usual expression for the standard deviation of the mean by a linear factor that also varies with  $n$  as shown in equation 8. The slope,  $m$ , and intercept,  $b$ , can be found by conducting a linear fit of the ratio between the observed standard deviation and the expected standard deviation (were the errors to have a normal distribution) for different numbers of averaged frames,  $n$ . This factor typically has the effect of increasing the error compared to that expected for a simple standard deviation of the mean.

$$\delta t_{p,ran} = \frac{s_p}{\sqrt{n}} (mn + b) \quad (8)$$

Infrared data sets of the form (T, x) or (T, y) are typically gathered by conducting a spatial average of temperature data that are oriented perpendicular to the direction of the data set. This spatial averaging will further decrease the random errors expressed by  $\delta t_{p,ran}$ . Equation 9 recommends a method for calculating the uncertainty in the mean temperature at location x,  $\delta t_{x,m}$ , for the number of temperature values extending in the y direction,  $N_y$ . Similarly, equation 10 recommends a method for calculating the uncertainty in the mean temperature at location y,  $\delta t_{y,m}$ , for the number of temperature values  $N_x$ .

$$\delta t_{x,m} = \frac{s_p}{\sqrt{N_y} \sqrt{n}} (mn + b) \quad (9)$$

$$\delta t_{y,m} = \frac{s_p}{\sqrt{N_x} \sqrt{n}} (mn + b) \quad (10)$$

Emittance and Background-Infrared temperature measurements require correcting for surface emittance and background thermal radiation and errors in these values will propagate. Equation 11 shows an expression for how the thermography system calculates a surface temperature,  $T_{IR}$ , from the total thermal radiation represented by the variable  $T_{e=1}$ , the emittance of the surface,  $e_{surf}$ , and the background radiation level represented by the variable  $T_{back}$ .  $T_{e=1}$  is an equivalent blackbody temperature for the surface being measured as defined in equation 5 above.  $T_{back}$  is an equivalent blackbody temperature for the background thermal radiation level. Values for both  $T_{e=1}$  and  $T_{back}$  are obtained from the imager by setting emissivity to unity. Equation 11 can be derived from equations 2 through 5.

$$T_{IR} = \left( \frac{(T_{e=1}^4 - (1 - e_{surf})T_{back}^4)}{e_{surf}} \right)^{1/4} \quad (11)$$

Errors in  $e_{surf}$  should be treated as a source of non-definable systematic uncertainty,  $\delta e_{surf}$ , and may be analyzed by propagating uncertainty in equation 1. Errors in  $T_{e=1}$  and  $T_{back}$  lead to uncertainties,  $\delta T_{e=1}$  and  $\delta T_{back}$ , that are subject to random uncertainty as described in equations 7,

8, 9, or 10. To analyze error propagation in equation 11 it is recommended to calculate the sum of the squares of partial differentials of equation 11 with respect to variables  $T_{e=1}$ ,  $T_{back}$  and  $e_{surf}$ . Equation 12 shows the form of such an expression for the uncertainty in  $T_{IR}$ ,  $\delta T_{IR}$ . A solution to equation 12 is shown in equation 13.

$$dT_{IR} = \sqrt{\left(\frac{\partial T_{IR}}{\partial T_{e=1}} dT_{e=1}\right)^2 + \left(\frac{\partial T_{IR}}{\partial T_{back}} dT_{back}\right)^2 + \left(\frac{\partial T_{IR}}{\partial e_{surf}} de_{surf}\right)^2} \quad (12)$$

$$dT_{IR} = \frac{1}{4} \left( \frac{T_{e=1}^4}{e_{surf}} + T_{back}^4 - \frac{T_{back}^4}{e_{surf}} \right)^{\frac{3}{4}} \left( \sqrt{\left(4 \frac{dT_{e=1}}{e_{surf}} T_{e=1}^3\right)^2 + \left(4 T_{back}^3 dT_{back} - 4 \frac{dT_{back}}{e_{surf}} T_{back}^3\right)^2 + \left(\frac{de_{surf}}{e_{surf}^2} T_{back}^4 - \frac{de_{surf}}{e_{surf}^2} T_{e=1}^4\right)^2} \right) \quad (13)$$

Field of View-A source of systematic error is potential variation in the imager's measurement performance across the field of view. It is recommended to conduct separate ancillary experiments with an isothermal, temperature-controlled plate to ascertain the uncertainty arising from variation across the field of view,  $\delta T_{FOV}$ . To conduct the experiments, fill the imager's entire field of view with the isothermal plate and record several thermograms with the maximum available amount of averaging over time (as many frames as possible) to reduce random errors. Then analyze every pixel, or thermographic data point, within the field of view for deviations from the mean of all the temperature values. It is recommended to conduct several such analysis with different view angles. The uncertainty,  $\delta T_{FOV}$ , is then determined from the magnitude of the largest deviations (maximum and minimum). When thermographic data are averaged over space, the uncertainty will be lower than it would be for an individual datum. Then the uncertainty could be determined from the standard deviation which may be calculated with equation 7.

Combination of Uncertainties-The total uncertainty should be estimated by combining the individual components described above. Equation 14 shows one method for estimating the total uncertainty in the final surface temperature,  $\delta T$ . Equation 13 can be used to obtain values for  $\delta T_{IR,smpl}$  and  $\delta T_{IR,Ref}$ . The uncertainty in the direct contact measurement of the reference emitter surface temperature,  $\delta T_{DC,Ref}$ , is determined from the system accuracy of the direct contact sensor combined with any errors associated with adjustments that correct for gradients in the surface material. The uncertainty arising from variations across the field of view,  $\delta T_{FOV}$ , is determined from the magnitude of deviations in heavily-time-averaged data for an isothermal plate that fills the section of the field of view being used.

$$dT = dT_{IR,smpl} + dT_{IR,Ref} + dT_{DC,Ref} + dT_{FOV} \quad (14)$$

Considering the overall complexity of the thermography system and its error analysis, it is recommended to perform a final check of errors by comparing data from a CTS experiment to referenced infrared temperature measurements of the CTS. The CTS is operated and measured as for surface conductance (discussed above and ASTM C 1199) with the main difference being that data are compiled for individual locations of temperature probe junctions. Location markers are useful for identifying probe junction locations in the thermographic data.

Spatial Coordinates-The uncertainty in spatial coordinates of the final data sets depend on imager resolution, viewing distance, magnitude of the real distance on the specimen surface, and resolution of the final data array. The resolution of the imager is determined by the instantaneous field of view, **IFOV**, which is a thermography equipment specification. The viewing distance, **D**, is the distance between the imager and the specimen at the time the thermogram was recorded. The distance on the specimen surface,

**H**, is a direct measurement of the distance between location markers used to identify the geometric region in the thermogram. The resolution of the data array is determined from the number of pixels in the array being analyzed, **N**. Equation 15 is one method for estimating the uncertainty in a spatial coordinate,  $\delta x$ .

$$\delta x = \sqrt{(D \tan(\text{IFOV}))^2 + \left(\frac{H}{N}\right)^2} \quad (15)$$

### Data Report

In addition to the final data sets, a complete report of data for a thermographic experiment should include: (1) a description of the test specimen and any modifications to its construction and/or emittance, (2) a description of the maskwall material and maskwall thickness, (3) location of surface temperature probes on the maskwall and the specimen, (4) orientation of the specimen in the maskwall and the direction of heat transfer, (5) orientation of the coordinate system used for spatial coordinates in the data sets, (6) approximate times when the chambers reached the setpoint temperatures and when the first thermogram was taken, (7) average air velocity and temperature on both sides of the specimen, (8) average surface temperatures for any surface probes on the maskwall or specimen, (9) surface emittance values used for the specimen, (10) background temperature levels measured with the background mirror, (11) center temperature and temperature span settings of the infrared imager for each thermogram, (12) temperature of the reference emitter measured with direct contact probes and corrections made for the surface temperature, (13) reference emitter surface emittance, (14) temperature corrections based on deviations between infrared and direct measurements of the reference emitter, (15) cold-side and warm-side mean radiative surface conductances, (16) cold-side and warm-side mean convective surface conductances, (17) overall mean surface conductances, (18) presence of condensation or frost on the specimen, and (19) indications of uncertainty for all data values.

### Conclusions

Documenting infrared thermography procedures and comparing measured and computer simulated data lead to the following conclusions and observations:

1. Quantitative infrared thermography can provide useful surface temperature data for comparison to computer simulations.
2. Reference emitter techniques are useful for improving the absolute accuracy of infrared temperature values.
3. Procedures are currently for flat specimens only because of limitations in properly correcting for background radiation.
4. Specimen surfaces need preparation with (a) low-emissivity location markers for accuracy of spatial values and with (b) high-emissivity coverings to raise the emissivity of surfaces that are too reflective.
5. Thermography combined with computer simulation is well suited for investigating *localized* surface conductance phenomena.
6. Procedures are currently not applicable to many designs of hot boxes because of physical interference between the radiation baffle and the viewing needs of the infrared imager; a thermography chamber must therefore be distinguished from a metering chamber.

### Acknowledgment

This work was supported by the Assistant Secretary for Energy Efficiency and Renewable Energy, Office of Building Technology, State and Community Programs of the U.S. Department of Energy under Contract No. DE-AC03-76SF00098.

## References

1. ASTM C 976, "Standard Test Method for Thermal Performance of Building Assemblies by Means of a Calibrated Hot Box," 1995 Annual Book of ASTM Standards, vol. 04.06, pp. 463-481, 1995.
2. ASTM C 236, "Standard Test Method for Steady-State Thermal Performance of Building Assemblies by Means of a Guarded Hot Box," 1995 Annual Book of ASTM Standards, vol. 04.06, pp. 52-62, 1995.
3. ASTM C 1199, "Standard Test Method for Measuring the Steady-State Thermal Transmittance of Fenestration Systems Using Hot Box Methods," 1995 Annual Book of ASTM Standards, vol. 04.06, pp. 658-669, 1995.
4. Sullivan, H.F., Wright, J.L., and Fraser, R.A., "Overview of a Project to Determine the Surface Temperatures of Insulated Glazing Units: Thermographic Measurements and 2-D Simulation," ASHRAE Transactions 102(2), American Society of Heating, Refrigerating and Air-Conditioning Engineers Inc., Atlanta, 1996.
5. Elmahdy, H., "Surface Temperature Measurement of Insulated Glass Units Using Infrared Thermography," ASHRAE Transactions 102(2), American Society of Heating, Refrigerating and Air-Conditioning Engineers Inc., Atlanta, 1996.
6. Griffith, B.T., Türler, D., and Arasteh, D.K., "Surface Temperatures of Insulated Glazing Units: Infrared Thermography Laboratory Measurements," ASHRAE Transactions 102(2), American Society of Heating, Refrigerating and Air-Conditioning Engineers Inc., Atlanta, 1996.
7. ASTM C 168, "Standard Terminology Relating to Thermal Insulating Materials," 1995 Annual Book of ASTM Standards, vol. 04.06, pp. 14-19, 1995.
8. ASTM C 1060, "Standard Practice for Thermographic Inspection of Insulation Installations in Envelope Cavities of Frame Buildings," 1995 Annual Book of ASTM Standards, vol. 04.06, pp. 565-570, 1995.
9. ASTM C 1153, "Standard Practice for the Location of Wet Insulation in Roofing Systems Using Infrared Imaging," 1995 Annual Book of ASTM Standards, vol. 04.06, pp. 641-646, 1995.
10. Griffith, B.T., Beck, F., Arasteh, D., and Türler, D., "Issues Associated with the Use of Infrared Thermography for Experimental Testing of Insulated Systems," Proceedings of the Thermal Performance of the Exterior Envelopes of Buildings VI Conference. American Society of Heating, Refrigerating and Air-Conditioning Engineers Inc., Atlanta, 1995.

## Appendix

This appendix contains details on certain equipment used at the author's infrared thermography laboratory, IRLab. These specific examples are intended to add detail to the general procedures discussed in the main body of the paper.

### *IR-Lab Climate Chamber*

The climate chamber used at the IRLab is a modified commercial food freezer, see Figure 2. Air flow is upwards and parallel to the maskwall, with a plenum (baffle) depth of 10 cm from the specimen surface. The entire air flow is routed through air ducts that have nearly constant cross-section size and rounded corners where the wind changes direction. Air leaving the blower circulates upward across the specimen, is

forced through the cooling coil, passes strip heaters, and then returns to the blower. The air blower is a custom-made, constant-speed, axial cross-flow fan with a diameter of 10 cm. that covers more than 95% of the entire plenum width. This design insures a uniform air velocity profile across the width and efficient operation with regard to cooling power requirements. Absolute air speed ranges between 3.9 and 6.0 m/s, depending on chamber operation and specimen geometry. Ice build-up on the cooling coil seems to be the cause of a gradual decrease in air velocity. A horizontal array of three separately controlled electrical strip heaters is installed between the cooling coil and the blower. Three separate zones (across the width) are controlled with instruments capable of  $\pm 0.05^\circ\text{C}$  accuracy. The overall surface conductance has been measured at  $30 \pm 5 \text{ W/m}^2\cdot\text{K}$ . Because of the high surface conductance, the temperature difference between air and the specimen surface is typically  $1^\circ$  to  $4^\circ\text{C}$ , depending on specimen properties and geometry, and the heat transfer from radiation to the plenum is low.

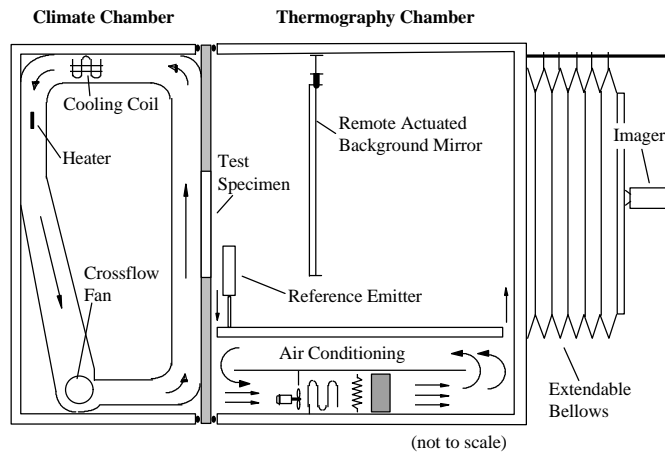


Figure 2. IRLab Thermography Chamber and Climate Chamber

### *IRLab Thermography Chamber*

The thermography chamber used at the IRLab has an outer size of 1.4 m wide and 2.1 m high with a depth that can vary from 0.9 to 4.2 m; see figure 2. It is a sandwich construction of sealed plywood and extruded polystyrene foam boards. Extendible bellows allow for an air-tight variable viewing distance. The imager is usually located outside the chamber and has an air-tight view port. Air circulation and conditioning equipment is located in a subfloor beneath the specimen and viewing enclosure. A 20-mm-wide intake slot runs across the entire width of the subfloor, creating an air sink which drains cooler air running off the specimen into the subfloor. On the opposite side of the subfloor a 44-mm-wide output slot introduces conditioned air at low velocity to the warm chamber. A recirculating air mixing chamber within the subfloor has much higher air velocities to improve heat exchange with the cooling coil and heaters. Five variable-speed fans force air through a custom-built heat exchanger cooled with temperature-controlled recirculating fluid. The slightly chilled air is then reheated by three individually controlled, flat-sheet heaters. A partition is used to recirculate most of the air back to the fan intake, bypassing the main chamber. The fan induced pressure differences between the intake and output slots cause a small volume of air to be exchanged with the warm chamber. The overall surface conductance has been measured from 7 to  $9.5 \text{ W/m}^2\cdot\text{K}$ , depending on fan power settings, but is usually close to  $8.0 \text{ W/m}^2\cdot\text{K}$ . The temperature difference between enclosure surfaces and the specimen is usually  $3^\circ$  to  $15^\circ\text{C}$ . Thermal radiation is about half of the total surface conductance.

### *IRLab Custom-built Reference Emitter*

One of the reference emitters currently used at the IRLab is a custom device based on a temperature-controlled liquid system, shown in Figure 3. One continuous fluid channel made of two concentric rectangular spirals with opposing direction is machined out of a solid block of copper leaving a 13-mm-thick solid portion directly underneath the reference surface. This design minimizes temperature gradients across the surface because heat is continuously exchanged between the liquid supply and return inside the block. A bore reaches to the center of the solid portion that accommodates a laboratory-grade, platinum resistance temperature probe (PRT) with a specified system accuracy of  $\pm 0.01^\circ\text{C}$ . The PRT probe runs parallel to the reference surface. Enough copper surrounds the bore that no discernible temperature gradients occur on the reference emitter surface. The backs of the fluid channels in the block are sealed with an additional copper plate. Except for the reference surface, the entire device and the liquid supply and return lines are insulated. A thin sample of the test specimen surface material is

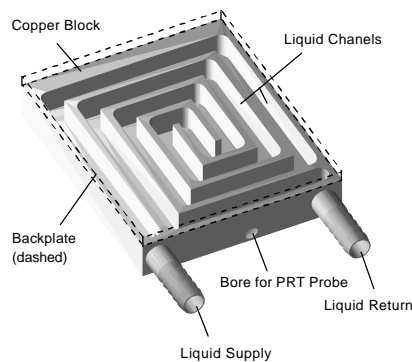


Figure 3. IRLab Custom-built Reference Emitter

mounted on the reference emitter with a heat sink compound. The temperature-controlled liquid is supplied by a recirculating bath with a built-in microprocessor controller. The finished assembly has much smaller outer dimensions than typical air-based commercial reference emitter making it less obtrusive in the thermography chamber. One disadvantage is a longer response time when changing temperature setpoint. The same temperature-controlled recirculating bath and laboratory grade PRTs are used to calibrate thermocouples and thermistors. Such a device can be built at approximately half the cost of a commercial blackbody reference emitter.

### *IRLab Error Analysis Example*

A sample analysis of error using real values from infrared temperature measurements conducted at the IRLab is provided as an example and to show that such measurements appear to show accuracies of  $\pm 0.5^\circ\text{C}$ . This example is for a  $5^\circ\text{C}$  span thermogram that was recorded using an average of 50 frames over time. The specimen and the reference emitter both have normal window glass as the surface material. The specimen emittance,  $e_{\text{surf}}$ , was determined using equation 1 with inputs  $T_{e=1,\text{smp}} = 308.2 \pm 2\text{K}$ ,  $T_{e=1,\text{ref}} = 308.8 \pm 2\text{K}$ ,  $T_{\text{back}} = 293.2 \pm 2\text{K}$ , and  $e_{\text{ref}} = 0.90 \pm 0.01$  (paper masking tape). The result from equation 1 and error propagation is  $e_{\text{surf}} = 0.86 \pm 0.01$ . Random errors are determined by applying equations 7, 8, and 13. The basic random error level calculated with equation 7; for this particular measurement it is  $\sigma_p = 0.20$ . For a fifty frame thermogram  $n = 50$  and equation 8 returns  $\delta t_{p,\text{ran}} = \pm 0.049^\circ\text{C}$  where  $m = 0.0136$  and  $b = 1.071$ . Emittance and background errors are determined with equation 13. The random uncertainty value  $\delta t_{p,\text{ran}} = \pm 0.049^\circ\text{C}$  is used for values of  $\delta T_{e=1}$  and  $\delta T_{\text{back}}$  in equation 13. Other inputs for equation 13

include  $T_{e=1} = 291.2\text{K}$ ,  $T_{\text{back}} = 294.3\text{K}$ ,  $e_{\text{surf}} = 0.86$ , and  $\delta e_{\text{surf}} = \pm 0.01$ . Equation 13 then returns  $\delta T_{\text{IR}} = \pm 0.072^\circ\text{C}$ . This uncertainty applies to infrared measurements of both the sample and the reference emitter, so  $\delta T_{\text{IR,smpl}} = \delta T_{\text{IR,Ref}} = \pm 0.072^\circ\text{C}$ . Uncertainty arising from performance variations across the field of view is estimated at  $\delta T_{\text{FOV}} = \pm 0.2^\circ\text{C}$ . Uncertainty in the direct contact measurement of the reference emitter surface is estimated at  $\delta T_{\text{DC,Ref}} = \pm 0.15^\circ\text{C}$ . Combining uncertainty using equation 14 yields a total estimate for the uncertainty in final temperature of  $\delta T = \pm 0.5^\circ\text{C}$ .